

## Temporal and thermal visualization by fusion of thermal images and 3D mesh

Emile Marie<sup>1</sup>, Vincent Lecomte<sup>1</sup>, Tania Landes<sup>1</sup>, H el ene Macher<sup>1</sup>, Chaimaa Delasse<sup>1,2</sup>

<sup>1</sup> Universit e de Strasbourg, INSA Strasbourg, CNRS, Laboratoire ICUBE UMR 7357, Equipe TRIO, 67000 Strasbourg, France

<sup>2</sup> Ecole des Sciences G eomatiques et de l'Ing enierie Topographique, Institut Agronomique et V et erinaire Hassan II, Madinat Al Irfane, 6202 Rabat, Maroc

(emile.marie, vincent.lecomte, tania.landes, helene.macher, chaimaa.delasse)@insa-strasbourg.fr

**Keywords:** Thermal Infrared, 3D Modelling, Data Fusion, Trees, Urban Climatology

### Abstract

In the context of the TIR4sTREEt (Thermal InfraRed for Street Trees) project, a huge measurement campaign has been organized. In order to study the interactions between trees and buildings regarding the surface temperature, thermal infrared (TIR) data have been acquired during a long period and from different points of view. Over a period of 17 days, the camera under study has been fixed on a mast and later, for specific days, on a low-cost mobile system. Several thousand images have been acquired. This paper introduces a methodology for creating a temporal thermal 3D model through the fusion of 2D thermal infrared images with 3D mesh models. The purpose of this fusion is to produce an efficient solution for visualization and analysis of detailed spatial and temporal variables like surface temperature. Therefore the temporal thermal 3D model is a faithful representation of reality and serves as a kind of reference model. Subsequently, validation of microclimatic simulation will be achieved by comparing the simulated surface temperature with the thermal reference model. First results show that the fusion is reliable and that this visualization solution is a robust and precious tool for facilitating the validation of microclimate simulation tools.

### 1. Introduction

The thermal study of buildings and trees plays a crucial role in urban climatology, providing a better understanding of the microclimate. Trees, thanks to their shading and transpiration, have the capacity to improve the diurnal urban comfort. The TIR4sTREEt project aims to deepen our understanding of the thermal interactions between street trees and their urban environment.

The study area is located in Strasbourg, covering three streets with three different tree species. The project is based on the analysis of microclimatic, geometric and thermal infrared data. However, the complexity of the related data presents a significant challenge in combining them in a manner that allows for exploitation in both spatial and temporal dimensions.

Furthermore, this research project aims to compare on site measurements with microclimatic simulations generated with the LASER/F (LAtent, SENSible, Radiation / Fluxes) tool (Kastendeuch et al., 2017). This tool is capable of simulating thermal interactions in a complex environment, facilitating urban microclimate studies. Therefore, it will help to predict the behavior of trees and their impact on the urban microclimate. Given that a large amount of thermal data has been acquired and should help to validate the simulations produced with LASER/F, a solution to automate the comparison must be developed. For the purpose of comparison, a methodology has been established to produce a temporal dynamic thermal model through the fusion of TIR images and a 3D mesh model of the site. This model will be employed to validate the results of microclimatic simulations, particularly with regard to surface temperature.

This raises a number of questions: given that thermal images are inherently 2D with low spatial resolution, how can thermal information be represented efficiently in a 3D model? How can

these results be visualized and suitable for simulation validation? Furthermore, how can processing be optimized and automated?

### 2. Related work

Usually, thermal images are analyzed in 2D. While useful, this approach has significant limitations, particularly when it comes to representing complex urban environments. Alternatively, 3D models offer more detailed visualization and richer data interpretation. With the advent of BIM (Building Information Modelling) and its wide-spread use in the field of surveying and construction, 3D digital models are becoming an indispensable medium. Simultaneously, thermal imaging is gaining increasing attention and driving numerous innovations, particularly in the field of sustainable development.

The literature presents several approaches for fusion of thermal information and 3D models. On the one hand, certain methodologies can be used to produce thermal point clouds, with specific applications in various contexts: for monitoring indoor environments (Macher et al., 2019) or building facades (Macher et al., 2022), and for representing thermal information on urban trees (Lecomte et al., 2022). While these approaches effectively depict complex geometries, they might not be the most efficient for comparison with simulations because the export format is not in adequation with the format of simulation outputs. On the other hand, it is possible to create 3D mesh models with thermal textures through UV mapping techniques, enabling the integration of thermal imagery (2D) into existing 3D models. Numerous studies have explored this approach: Iwaszczuk and Stilla (2016) applied UV mapping to generate TIR textures on 3D building models, Lagu ela et al. (2013) developed thermal texturing for BIM models, and Paziewska and Rzonca (2022) investigated combining thermal and RGB data collected via drone for texturing a church. However, in most cases, thermal information remains limited to simple visualization purposes, serving

primarily as an informational overlay without temporal consideration. This sets the stage for more advanced applications, such as those described by Lee et al. (2013), where temperature data are leveraged for temporal analysis and comparative purposes.

Regarding comparison, Lee et al. (2013) compared 3D simulation results from LASER/F with rectified 2D thermal images by essentially projecting the 3D vertices of a mesh onto a 2D raster image domain. The temperature value of each triangle was derived from the average temperature of its corresponding pixels. This allowed for a triangle-by-triangle comparison and enabled validation of the simulation model using a process that could be described as the inverse of the UV mapping technique. However, this approach reduces the advantages of 3D analysis, limiting the ability to fully explore spatial interactions within the urban environment.

### 3. Dataset

A large dataset was acquired throughout the project: TIR images acquired from a fixed position and from a mobile system, punctual surface temperature measurements data and geometric data. Using more than 5000 TIR images and a previously reconstructed 3D model, a thermal reference model will be created.

#### 3.1 TIR images acquired from a fixed position

A data acquisition campaign was carried out during the summer of 2023 over 17 days. When considering specifically the period from July 18 to July 23, a total amount of 1,728 TIR images are concerned. The images were taken from a fixed viewpoint on a 6 meter-high mast, providing a high-angle perspective that encompasses sections of the façade, trees, ground and hedges (Figure 1).

The thermal images were acquired using a FLIR T560 camera, with key specifications outlined in Table 1. The camera is equipped with thermal sensor and Red-Green-Blue (RGB) sensor, enabling simultaneous acquisition of thermal and RGB images, with a fixed lever arm. The TIR camera measures the radiation emitted by the object, which is then converted into surface temperature. This measurement can be adjusted for factors such as distance, emissivity, humidity, etc.

Regarding acquisition settings, a pair of thermal and RGB images was taken every five minutes. This interval was chosen to allow the detection of physical phenomena occurring in the study area, while balancing storage space considerations (Fox et al., 2012).

#### 3.2 TIR images acquired from a mobile system

In a second phase, a mobile acquisition system was developed to extend the acquisition to a wider part of the scene than the single façade observed by the fixed camera. Moreover, the cart was used at key times of the day, including dawn, zenith, and twilight. This enables the monitoring of temporal variations of the surface temperature during the warm days.

The mobile system is equipped with the same FLIR T560 camera, positioned equidistantly between two wide-angle GoPro cameras (Table 2) to form a stereoscopic system. The latter is mounted on a bar, itself mounted on a telescopic tripod fixed on

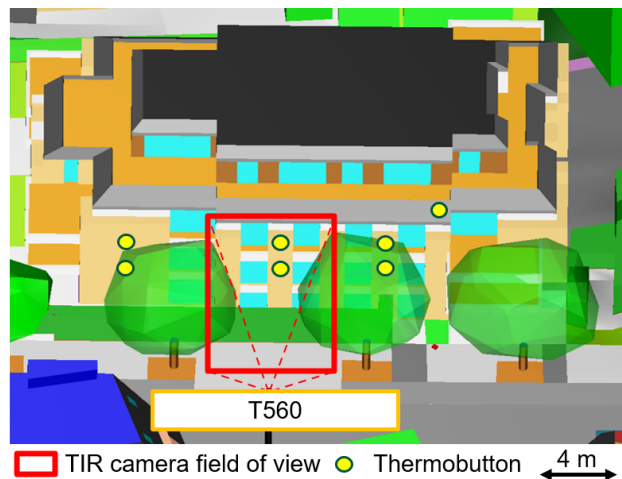


Figure 1. Perspective view of the 3D model with a focus on the area covered by the FLIR T560 acquisitions

Camera Model	FLIR T560
Image Format	4:3
Infrared Image File Format	Infrared JPEG
Field of View	42° x 32°
IR Image Resolution	640 × 480 pixels
RGB Image Resolution	1280 × 960 pixels
Spectral Range	7.5 to 14 μm
TIR Pixel Size	12 μm
TIR Focal Length	9.7 mm
RGB Focal Length	3.4 mm
Accuracy	±2 °C
Temperature Range	-20 °C to 120 °C
Thermal Sensitivity / NETD	< 40 mK

Table 1. Specifications of the FLIR T560 Camera

a mobile cart. The mobile nature of this setup enables the acquisition of image "quadruplets" (two GoPro images, one FLIR TIR image, and one FLIR RGB image) at a constant height from the ground.

Acquisitions were conducted in the study area during the summer, at three times a day (dawn, noon, and dusk) as shown in Lecomte et al. (2024). Each acquisition followed the same path within the study area, covering the trees and buildings of interest from various viewpoints and distances. Each acquisition phase lasted approximately one hour, capturing around 120 image quadruplets at 30-second intervals between each acquisition. The use of wide-angle cameras, along with the strategic orientation and placement of the various sensors, provides significant overlap between the different shots, facilitating the subsequent orientation of thermal images necessary for creating thermal textures.

Camera Model	GoPro Hero 4
Image Format	4:3
Image File Format	JPEG
Field of View (FOV H)	122°
Photo Resolution	12 MP (3000 × 4000 pixels)
Aperture	f/2.8
Photo Focal Length	3 mm
Dimensions	41 mm x 59 mm x 30 mm

Table 2. Specifications of the GoPro Hero 4 Camera

### 3.3 Geometric data

A 3D model of the study site was already available from laser-scanning processing. This model is used as the basis for further projection of TIR images and generation of 3D thermal models. The 3D model is a meshed structure with a Level of Detail (LOD) of 3 for buildings of interest, featuring facets of varying sizes.

Since the ultimate objective of this approach is to compare measured surface temperatures to those simulated by LASER/F, it is imperative to ensure that the decimation level chosen for constructing the temporal thermal reference model matches that used in the simulations. Thus, the decimation level was selected to keep calculation times within a reasonable range, both for processing the 3D and TIR data fusion, as well as for micro-climate simulations, as they can result in extended computation periods, sometimes lasting several days. To analyze the thermal dynamics of the area more precisely, the mesh was decimated to a resolution of 0.05 square meters, resulting in a model with approximately 614,000 facets. For instance, the mesh corresponding to the area observed from the fixed camera contains around 2,200 facets while the mesh for the area covered by the mobile acquisitions contains 14,000 facets.

Additionally, to facilitate and automate the georeferencing of data acquired with the mobile cart, a previously accurately georeferenced photogrammetric block (based on high resolution cameras) of the study area, was used.

### 3.4 Punctual surface temperature data

To validate the surface temperatures acquired by the TIR images, thermobuttons were placed on the building. These thermobuttons are coin-sized surface temperature recorders and are more accurate in comparison with thermal images, providing punctual temperatures with 0.5 °C accuracy.

Thermobuttons provide contact-based measurements of surface temperature, while the TIR camera delivers 2D images. In our study, the thermobuttons were set to record a measurement every fifteen minutes.

Together, these complementary data sources enhance the quality of the thermal validation and provide a stronger foundation for further analysis using the thermal reference model.

## 4. Developed methodology

In this section, the general methodology to create a thermal reference model from TIR images acquired from a fixed position will be developed. Then, the methodology will be adapted to mobile acquisitions. An additional challenge is that this representation must be presented in a format that is consistent and comparable to that of the simulation output.

### 4.1 General approach

Automation is an essential issue, given the large volume of data collected over extended acquisition campaigns, often spanning several months and recording approximately 300 infrared thermal images daily, as seen with the fixed viewpoint acquisitions. Thus, significant effort has been invested in optimizing processing times, simplifying, and automating the workflows.

After several experiments, the main steps of the processing chain developed for creating the temporal thermal model are presented in figure 2 and will be detailed in the following paragraphs.

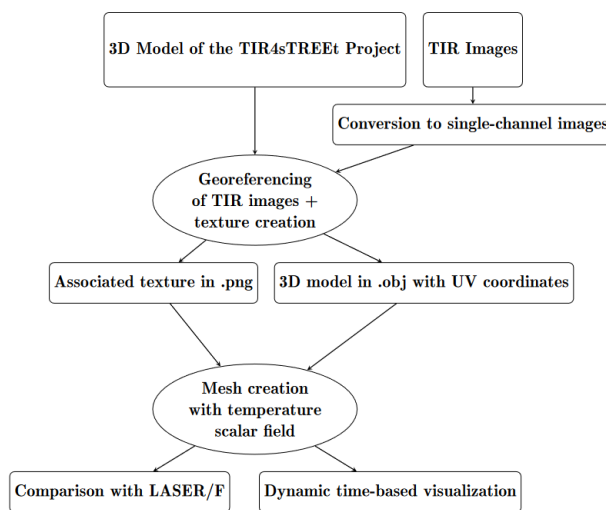


Figure 2. Flow chart

### 4.2 Data pre-processing

Initially, it is necessary to process the output files from the TIR camera, as the raw files are multi-channel radiometric images. We are specifically interested in the layer containing temperature values. The TIR image corresponds to a temperature matrix which can be viewed using a colour scale.

For subsequent processing, temperature matrices need to be extracted in .csv format. From these matrices, single-channel images are reconstructed to simplify the creation and use of thermal texture files. To automate this step, a Python program coupled with the FLIR Software Development Kit (SDK) and the PIL python library has been developed. Additionally, for each image, temporal metadata is stored to enable temporal visualization and analysis.

To ensure compatibility with the subsequent processing steps and software, the chosen solution converts the temperature values into centikelvins. This provides a range from 0 to 65,536 centikelvins, equivalent to -273.15 °C to 382.21 °C, deemed sufficient for this study. Furthermore, as each degree is coded over one hundred values, the precision uncertainty is limited to one hundredth of a degree, preventing any data loss in these conversions.

### 4.3 Alignment of TIR images

In order to enable the merging of the TIR data with the 3D model by texture creation, the external orientation parameters of TIR images must be calculated to match the coordinate system of the 3D model. The fact that thermal images are automatically registered with RGB images is an advantage for the relative orientation of the set of images. Indeed, the raw TIR files from the FLIR T560 are low-resolution images (Table 1) compared to the corresponding RGB images. Therefore, it is common practice to orient the RGB images first, and then deduce the relative orientation of TIR images. To achieve this, the orientation of the RGB photos is determined using control

points. A calibration performed in MATLAB provided the intrinsic parameters of the TIR camera, as well as the translation and rotation parameters between the RGB and TIR sensors (Macher et al., 2022). Then, using the relative translation and rotation parameters between the RGB and TIR sensors, the orientation of TIR images was deduced.

#### 4.4 Creation of thermal texture by UV mapping

Once the single-channel images are obtained and the TIR cameras are georeferenced, the next step is texture creation. The oriented TIR images are projected onto the model, enabling texture generation. This step is achieved using the photogrammetry software Metashape (Agisoft).

In some difficult cases, an RGB texture is used to visually control the registration of the images. RGB textures are preferred because thermal textures, being in grayscale, limit visual control. RGB textures additionally make it easier to identify areas where masks should be applied. Generally, the masks are applied to elements not represented in the 3D model.

It should be noted that the reconstruction process keeps the original radiometric values, with no blending or hole-filling in the texture. This is made to ensure data values are not distorted. Once this step is complete, the 3D model is assigned UV coordinates. These coordinates will be used in next section to create scalar fields, linking the mesh to an image (texture file).

#### 4.5 Creation of a mesh with scalar fields

Once the texture files and the 3D model with UV coordinates are ready, each facet of the mesh is processed to retrieve the corresponding pixel values from the textures using the UV coordinates. This process involves segmenting the thermal texture based on the UV map, where each facet of the mesh corresponds to a specific region of the texture. Since the values were previously converted to centikelvins and encoded in 16-bit, only a reverse conversion is necessary for each facet. This enables accurate mapping of thermal values onto the mesh based on the segmented texture regions.

Each triangle therefore corresponds to a series of temperature data. From this data, it is possible to create a mesh with various scalar fields, one representing the thermal information itself and others characterizing additional data attributes.

The first layer contains the average of the pixels within each facet (Fig. 3). The second layer refines this by averaging pixel values after removing outlier values. This filtering excludes values exceeding three standard deviations from the mean as well as any null values (-273.15 K). Such filtering is necessary, as facets along the edges are only partially covered by the texture and therefore do not provide meaningful information at the level of decimation used, as seen in figure 3. Consequently, when the proportion of null values within a facet is too high, the standard deviation under the three-sigma rule will not effectively eliminate outliers, as it is already skewed by an excessive proportion of extreme values (-273.15 K) (Fig. 4).

A third scalar field provides the percentage of null values within a facet, as explained earlier. This field better characterizes the source of the standard deviation in unfiltered facets, indicating whether the standard deviation reflects actual variation within the facet due to high temperature inhomogeneity, or if it represents edge effects due to mesh topology. Depending on the

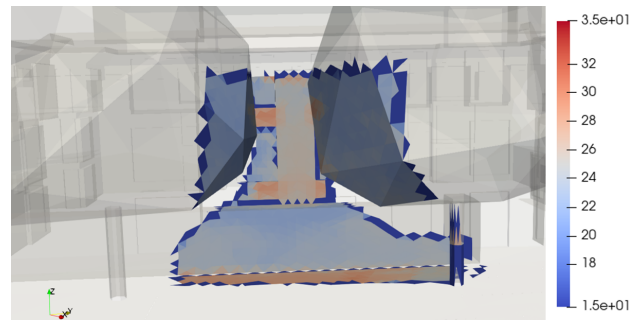


Figure 3. Visualization of raw temperatures (in °C)

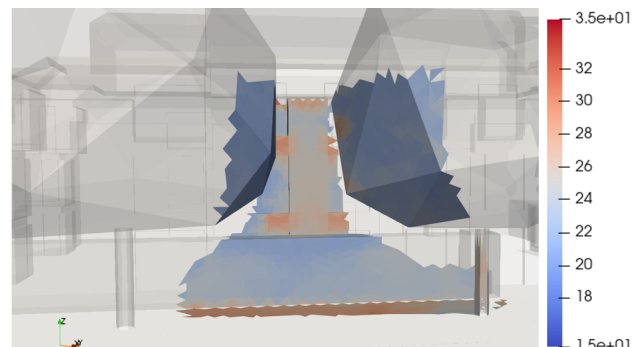


Figure 4. Visualization of filtered temperatures (in °C)

specific case, the acceptable maximum proportion of null values must be chosen accordingly

Many facets along the edges (trees, hedges, etc.) exhibit anomalous averaged values (below 0 °C, appearing as dark blue facets in Figure 3) due to unassigned pixels (mesh facets straddling between the camera's field of view and areas not visible to it). Notably, thanks to our filtering protocol, these anomalous values are less prevalent than in the visualization of raw temperatures, allowing us to recover information along the edges.

#### 4.6 Thermal visualization

The Paraview (Kitware) software's ability to handle scalar fields and manage the temporal dimension makes it suitable for this study. It enables the temporal visualization and analysis of a mesh containing different layers of information for each facet. Paraview's features, coupled with the addition of scalar fields and temporal data, make the results easily exploitable and facilitate comparisons with simulations.

Furthermore, this method, initially developed for acquisitions from a fixed viewpoint, has been generalized for mobile acquisitions as well.

#### 4.7 Method generalization to mobile acquisitions

To process data collected from the mobile system, new steps must be added to the processing chain to orient the thermal images from the mobile system. This step was straightforward for the fixed viewpoint, where the camera orientation remained constant over time, unlike the case with mobile acquisitions.

Below, we will detail the modifications made to process the mobile platform data. The flow diagram provides a brief overview of the various processing steps (Figure 5).

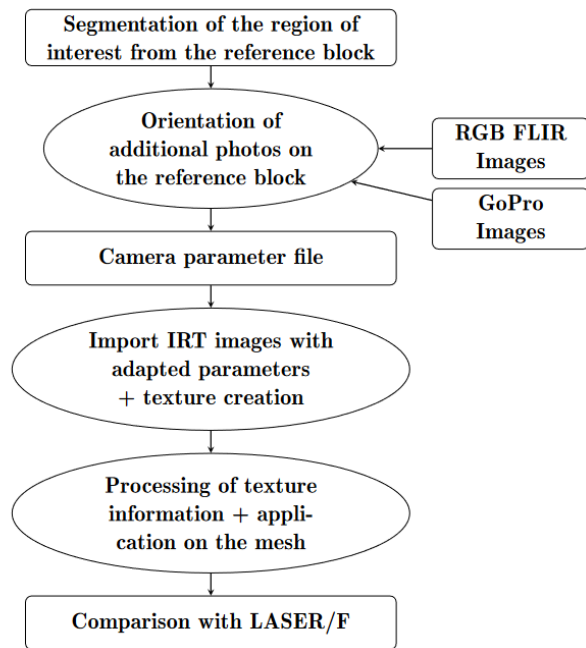


Figure 5. Flow chart developed for the fusion of thermal images and the 3D model in the case of mobile acquisition

The data used in this section are sourced both from the mobile cart and the reference photogrammetric block. The processing steps are as follows:

- An area of interest : (which corresponds to a building, or a small portion of the loop made with the cart) and all the associated oriented photos are extracted from the reference photogrammetric block. Building-scale blocks, typically containing about ten photos or less than five minutes of data, are used. This time frame ensures the acquisition area remains thermally stable during the data collection (Lehmann et al., 2013).

- Image selection : Only the photos covering the area of interest, previously extracted from the reference block, are selected from cart photos. This selection helps to reduce the number of files and thus significantly speeds up processing times. Each cart passage (three per day) generates a sequence of "quadruplets" of images. Thus, a Python program is employed to select the images to keep from one of the four folders related to a cart passage and import all the corresponding quadruple of images.

- Import and orientation: The photos are then imported and oriented using Metashape, with default settings except for "generic preselection". This setting, typically used to speed up processing, aligns matching images in two steps by first detecting tie points on downsampled images, then refining these points at full resolution. However, since the RGB FLIR photos are of relatively low quality (1280 x 960 pixels), this setting is disabled to maximize the detection of correspondences. The block of RGB photos is oriented and fixed in position, after that, the FLIR RGB images are overlaid to complete the alignment process.

- Extracting and adjusting orientation parameters: After orientation, the camera parameters are extracted. A Python program then replaces the RGB image names with their thermal infrared counterparts, applying offset corrections for sensor alignment. The cart TIR images are also converted into single-channel images, consistent with the method applied to the fixed TIR image dataset.

Finally, the remainder of the method is applied, and the temporal thermal models are created.

## 5. First results

Before proceeding with further analyses, it is necessary to evaluate the quality of the camera orientation and the thermal information. The following subsections outline two complementary evaluation approaches.

### 5.1 Quantitative evaluation of camera orientation

The orientation of thermal infrared images was achieved using a spatial resection method based on ground control points, mainly positioned at window corners. Additional control points were selected at other corners for improving accuracy. The points were marked both on the 3D model and on the thermal images. However, the limited resolution of the thermal images, along with the halo effects from radiation, introduce some challenges in precise marking.

Despite these limitations, the deviations of control points remain moderate, with an average error of 2.7 cm. Additionally, one point among the seven selected shows a larger deviation (6.3 cm), skewing the average slightly due to marking errors. After removing this extreme value, the average deviation is 2.1 cm. This quantitative assessment aligns the visual analyses conducted with RGB textures.

Given the facet size of  $0.05 \text{ m}^2$ , these deviations will not compromise the accuracy of subsequent analyses and comparisons with simulations.

### 5.2 Quantitative evaluation of thermal information

To assess the quality of thermal information applied to the 3D model, comparisons with "reference" sensors, deemed more accurate and reliable than the infrared thermal camera, are necessary. A facet of the mesh within the study area was matched to a thermobutton placed on the facade. The figure 6 illustrates the behavior of this mesh facet, with data extracted from thermal infrared images via their corresponding texture files, alongside the raw measurements from the thermobutton.

As observed in Figure 6, the temperature variations are largely similar, with a standard deviation of  $0.9 \text{ }^\circ\text{C}$  between the two series. The thermobutton consistently registers a higher temperature than the camera-derived data, with respective mean values of  $23.6 \text{ }^\circ\text{C}$  and  $22.9 \text{ }^\circ\text{C}$ .

Additionally, when using a conventional method of a region of interest (ROI) directly from the TIR images (selecting a specific portion of the thermal image corresponding to the thermobutton and averaging the pixel values within this area), the resulting temperature curve aligns almost perfectly with the surface temperature curve extracted from the thermal model. The mean temperature of the ROI is  $22.9 \text{ }^\circ\text{C}$ , identical to the mean temperature of the facet matched to the thermobutton. The standard deviation of the differences between these two data series is  $0.03 \text{ }^\circ\text{C}$ . This minimal deviation, given the measurement precision of the used devices, indicates that the two series are almost identical.

Consequently, each model facet can be treated as equivalent to an ROI, thereby validating the thermal content of the facets in the digital model. The model leverages the entire thermal image, enabling automated visualization and reliable comparison with simulation results.

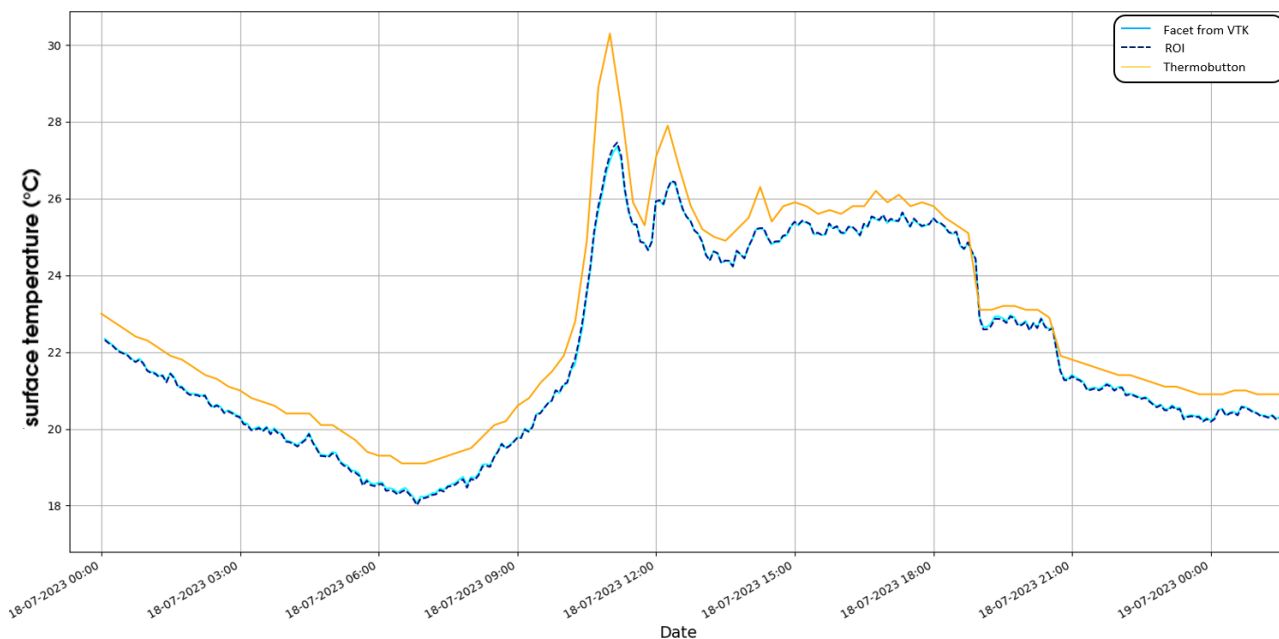


Figure 6. Comparison of surface temperatures between the thermobutton, the corresponding facet on the thermal reference model, and a region of interest (ROI) on the TIR image from the day of 18-07-23

### 5.3 Thermal reference model from the fixed camera

The methodology was applied to all the images collected during the acquisition campaign. Figure 9 shows an example of a thermal reference model based on a photo taken on 19/07/2023 at 10:14 A.M. The corresponding RGB image (Figure 8) provides a clearer way to see the ROI, revealing details such as the shadow cast by the tree on the facade. Thermal effects are visible both on the TIR image (Figure 7) and on the mesh model (Figure 9), where blue facets represent areas still in shadow, while red facets indicate areas being heated. As the shadow fades due to the sun’s movement, the red facets continue to warm up.

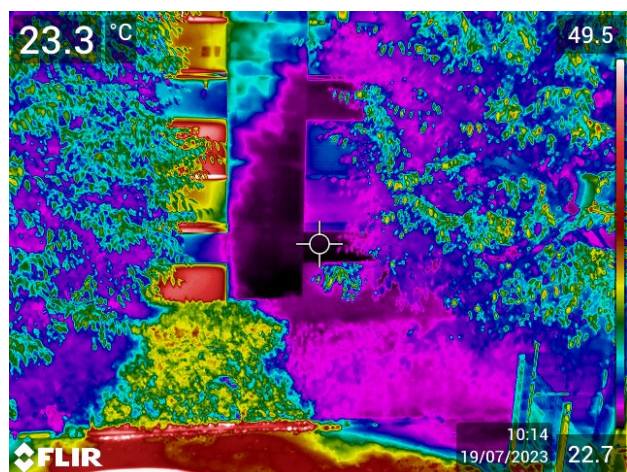


Figure 7. example of a TIR image used for the reference model



Figure 8. the RGB image corresponding to the captured thermal image from Figure 7

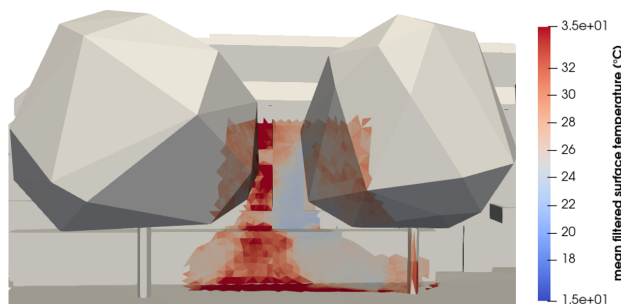


Figure 9. Reference thermal model (in grey unassigned values, in colors facets containing thermal data)

### 5.4 Thermal reference model from the mobile camera

The result obtained by applying the processing chain described in Figure 5 on 22 images taken along a building is shown in Figure 10. The height of the bar supporting the cameras made

it possible to scan a part of the building’s second floor, including the slab. At this stage, many applications are possible, such as the analysis of thermal bridges on concrete slabs in buildings.

But above all, this approach enhances the surface available for comparison with simulations at specific moments in time, including dawn, zenith, and twilight.

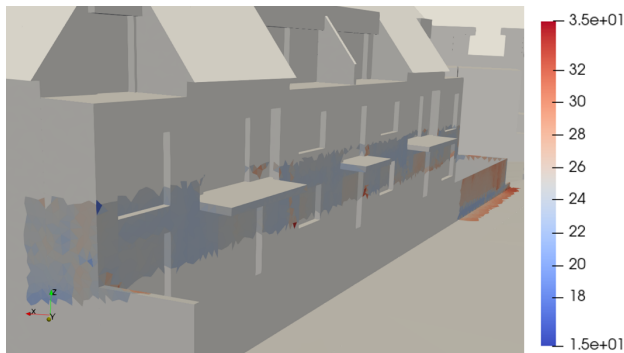


Figure 10. Reference thermal model with mean filtered surface temperature (in °C)

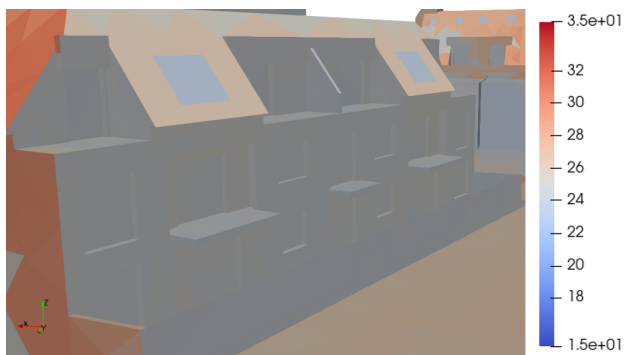


Figure 11. Simulated Surface Temperatures (in °C) on LASER/F on 08/21/2023 at 6:00 AM

In Figure 11, we can see a simulation output of surface temperatures generated by LASER/F. Since the format is identical to the reference thermal model, comparisons will be straightforward.

## 6. Perspectives

Currently, the orientation of the thermal camera on the mobile system is achieved by aligning the RGB images with a georeferenced photogrammetric block. For the twilight acquisitions, the GoPro images align well on the photogrammetric block, whereas the FLIR RGB images yield less satisfactory results due to increased noise from its lower-quality RGB sensor. To address this issue, it would be beneficial to fix the position of the FLIR RGB sensor relative to the two GoPros, addressing the issue of relative calibration. This approach would involve constraining known variables, such as the lever arms of the cart, and determining the position of the other cameras in relation to a global reference frame, thus improving the overall alignment of the thermal and RGB images.

A second improvement involves masking objects in mobile acquisitions that are not present in the 3D model. Currently, foreground elements, such as cars and fences, are masked manually to prevent their projection onto the 3D model. This step could be optimized by automatically segmenting thermal images using advanced segmentation models, such as the Segment Anything Model (SAM).

## 7. Conclusion

In this paper, an innovative and robust method for producing temporal thermal 3D models based on fixed and mobile thermal measurements has been developed. Two processing chains have been proposed and assessed geometrically and radiometrically. The fusion of thermal 2D data with 3D models facilitates the visualization and therefore the analysis of information that is variable in time and in space, like surface temperature. The transition from a 2D to a 3D representation using this methodology allows to keep the raw data, without degrading it.

Another major advantage of the proposed method is that each facet of the 3D model can be considered as a ROI. As the 3D simulation model is based on the same geometric mesh, the thermal reference model can automatically be compared with the simulation results. This is of great interest for research in the field of climatology, where simulation deliverables need to be validated.

## 8. Acknowledgments

The authors would like to thank the Agence Nationale de la Recherche (ANR) for supporting the project TIR4sTREEt (ANR- 21 CE 22 0021).

## References

- Iwaszczuk, D., Stilla, U., 2017. Camera pose refinement by matching uncertain 3D building models with thermal infrared image sequences for high quality texture extraction. *ISPRS Journal of Photogrammetry and Remote Sensing*, 132, 33–47.
- Kastendeuch, P. P., Najjar, G., Colin, J., 2017. Thermo-radiative simulation of an urban district with LASER/F. *Urban Climate*, 21, 43–65.
- Lagüela, S., Díaz-Vilariño, L., Martínez, J., Armesto, J., 2013. Automatic thermographic and RGB texture of as-built BIM for energy rehabilitation purposes. *Automation in Construction*, 31, 230–240.
- Lecomte, V., Macher, H., Landes, T., 2022. Combination of thermal infrared images and laserscanning data for 3D thermal point cloud generation on buildings and trees. *The International Archives of the Photogrammetry, Remote Sensing and Spatial Information Sciences*, XLVIII-2/W1-2022, 129–136. <https://isprs-archives.copernicus.org/articles/XLVIII-2-W1-2022/129/2022/>.
- Lecomte, V., Macher, H., Landes, T., Nerry, F., Cifuentes, R., Kastendeuch, P., Najjar, G., Delasse, C., 2024. Thermal measurement campaign in three streets of Strasbourg to study interactions between trees and facades. <https://www.sft.asso.fr/DOIeditions/CFT2024/Abstracts/p79.html>. Publisher: Société Française de Thermique.
- Lee, D., Pietrzyk, P., Donkers, S., Liem, V., van Oostveen, J., Montazeri, S., Boeters, R., Colin, J., Kastendeuch, P., Nerry, F., 2013. Modeling and observation of heat losses from buildings: The impact of geometric detail on 3D heat flux modeling. 353–372.
- Macher, H., Boudhaim, M., Grussenmeyer, P., Siroux, M., Landes, T., 2019. Combination of thermal and geometric information for BIM enrichment. *The International*

*Archives of the Photogrammetry, Remote Sensing and Spatial Information Sciences*, XLII-2/W15, 719–725. <https://isprs-archives.copernicus.org/articles/XLII-2-W15/719/2019/>.

Macher, H., Landes, T., 2022. Combining TIR images and point clouds for urban scene modeling. *The International Archives of the Photogrammetry, Remote Sensing and Spatial Information Sciences*, XLIII-B2-2022, 425–431.

Paziewska, J., Rzonca, A., 2022. Integration of Thermal and RGB Data Obtained by Means of a Drone for Interdisciplinary Inventory. *Energies*. <https://api.semanticscholar.org/CorpusID:250365867>.